Numerical investigation of wave propagation and transformation over a submerged reef

Jinxuan Li[1,2,*], Jun Zang[2], Shuxue Liu[1], Wei Jia[1], Qiang Chen[2]

[1]*State Key Laboratory of Coastal and Offshore Engineering, Dalian University of Technology, Dalian, China*

[2]*WEIR research unit, Department of Architecture and Civil Engineering, University of Bath, Bath, UK*

*Lijx@dlut.edu.cn

Numerical investigation of wave propagation and transformation over a submerged reef

In this paper, wave transformation over a submerged reef has been numerically studied based on the OpenFOAM model. This numerical model solves the Reynolds-Averaged Navier-Stokes equations for two-phase flow, and employs the volume of fluids (VOF) method for the free surface. The *k-ω* SST turbulence model is used to simulate wave breaking and the wave generation library *waves2Foam* is adopted to generate waves in the model. The numerical model is first validated against the physical experimental data, and it is shown that the model is capable of simulating the key processes of wave shoaling, breaking and transmission over the submerged reef. Then, a series of numerical tests are conducted considering different incident wave heights, submergences and slopes of the reef. The influences of reef slope and submergence on the wave properties over the reef are discussed, which include the wave reflection and transmission coefficients, breaking wave height, wave induced setup and energy dissipation.

Keywords: Wave transformation; Wave breaking; OpenFOAM

1. Introduction

In the recent years, with increasing maritime activities in reef region, such as tourism, fishery, navigation aid, *etc*., some engineering works were built on the reef. While, the hydrodynamic environment caused by the special bathymetry of the reef is not fully clear. Reefs are characterized by a steep slope and a shallow platform attached. As waves propagate from deep water to reefs, the rapid decreasing of water depth causes wave reflection, shoaling and breaking. The hydrodynamics of these complex processes are different from those occurring in gentle or mild slopes, and some existing formulas (such as wave breaking criteria) will not be suitable. In order to support the engineering design and better protect the environment of the reef region, a comprehensively understanding of the process of wave propagating over submerged reef is essential.

Numerous studies have attempted to investigate the wave environment on submerged reefs. Some field measurements of wave properties over a reef are obtained by Young (1989), Hardy and Young (1991), Massel and Brinkman (1999) and Lentz et al. (2016). But most of the studies are conducted in experimental laboratory. In these tests, the reef profile is considered as an incorporation of a steep reef-face and a reef plat with shallow water depth. Jensen (1991) conducted an experiment to study the wave transformation and water level on a reef with slope 1:1. Gourlay (1994) preformed experiments to investigate the wave breaking on the reef bathymetry with slope 1:4.5. Recently, Yao et al. (2013) conducted a series of laboratory experiments to study the characteristics of wave breaking over fringing reefs. In addition, Smith and Kraus (1991), Blenkinsopp and Chaplin (2008) and Lee et al. (2014) also studied the different aspects of wave properties on reef bathymetry.

It is difficult to consider too many factors in physical experiments, due to the inconvenience and relatively high cost. In this sense, numerical simulation provides an alternative to investigate systematically the wave properties on reef. The typical models used in the literature are based on the Boussinesq-type equation (Peregrine, 1967; Madsen and Sørensen, 1992; Nwogu, 1993). These models reduce the three-dimensional problem to two-dimensional problem by using the polynomial approximation to the vertical direction of the velocity field, and thus have high accuracy and computational efficiency (Karambas and Koutitas, 2002; Lynett et al. 2010; Kim, 2015; Kirby, 2016). Skotner and Apelt (1999) first used the Boussinesq model to simulate the regular waves propagating onto a submerged coral reef consisting the relatively steeper slopes (1:10.6). Later, Nwogu and Demirbilek (2010), Yao et al. (2012) and Fang et al. (2014) developed variant forms of Boussinesq model to investigate the wave properties on reefs with various profiles, respectively.

However, wave breaking is a complex physical process which involves the air-water interaction, overturning motion and vortex generation. While, in Boussinesq models, a predefined empirical energy dissipation is usually used to deal with energy dissipation caused by wave breaking, and no turbulence model is considered. Therefore, it cannot simulate free surface overturning or fully describe the complex breaking process. So, the Navier-Stokes equations considering turbulence model are more suitable for this kind of simulation (Lin and Liu, 1998; Torres-Freyermuth et al., 2010; Chen et al., 1999; Hieu et al., 2004; Wang et al. 2009; Jacobsen et al. 2012; Alagan Chella et al., 2015). Lin and Liu (1998) simulated the wave shoaling and breaking on a gentle slope by solving the Reynolds equations and k-ε equations. Xie (2012) developed a two-phase flow model based on Reynolds-Averaged Navier-Stokes equations with the k-ε turbulence model. He simulated the breaking waves in deep and shallow water, including wave pre-breaking, overturning and post-breaking processes. Hieu et al. (2004) developed a two-phase flow model based on Navier-Stokes equations and large eddy model and simulated the wave propagation in shallow water. All of these studies demonstrate that the Navier-Stokes approach is well suitable to simulate the wave breaking process.

OpenFOAM, an open source CFD software, provides a large number of solvers and utilities to cover a wide range of problems. It is one of the widely used CFD models in coastal and offshore engineering applications (Morgan et al. 2010; Higuera et al. 2013; Jacobsen and Fredsoe 2014; Chen et al. 2014; Devolder et al. 2018). Jacobsen et al. (2012) extended the OpenFOAM model and developed the Waves2Foam, which is a toolbox for wave generation and absorption. Morgan and Zang (2011) simulated the regular wave propagation over a submerged bar based on OpenFOAM model. The numerical results agree very well with the experimental measurements, including both

wave forms and wave amplitude spectra—up to 6^{th} order harmonics have been correctly simulated. Higuera et al. (2013) simulated the focusing wave group propagating over a bathymetry with slope 1:20. The wave group was extraordinarily well captured during the propagation, shoaling and breaking process. Chenari et al. (2015) studied the regular wave propagation and breaking on slope based on Waves2Foam. Osorio-Cano et al. (2018) developed a CFD model based on OpenFOAM and analysed the hydrodynamics related to wave energy dissipation over a coral reef. Their studies presented OpenFOAM as powerful software which could be used in coastal and ocean engineering.

For better understanding wave properties on the special reef bathymetry, especially the reef slope's affects which is inconvenient and expensive for physical model tests, numerical modelling with Waves2Foam is used to simulate wave propagation over a submerged reef in this present paper. The model is first validated by comparing the numerical results with experimental data. Then, a series of numerical simulations are conducted considering different wave heights, submergences and slopes. The reflection coefficient and transmission coefficient, wave setup, breaking wave height and energy dissipation are discussed in detail. The analysis focuses on the influence of reef slope and submergence on wave properties. Finally, the conclusions are drawn, which will help with structure designs in the reef region and better understanding of the waves propagating to the coast.

2. Numerical Model

2.1 Governing equations

The governing equations in the current numerical model for two-phase incompressible flows are the Reynolds-Averaged Navier-Stokes equations:

$$\frac{\partial \rho \mathbf{u}}{\partial t} + \nabla \cdot [\rho \mathbf{u}\mathbf{u}^T] = -\nabla p + \rho \mathbf{g} + \nabla \cdot [\mu \nabla \mathbf{u} + \rho \boldsymbol{\tau}] \quad (1)$$

$$\nabla \cdot \mathbf{u} = 0 \quad (2)$$

Here, $\mathbf{u}=(u, v, w)$ is the velocity field, p is the pressure, ρ is the density, $\mathbf{g}$ is the gravitational acceleration and μ is the dynamic viscosity. $\boldsymbol{\tau}$ is the specific Reynolds-stress tensor:

$$\boldsymbol{\tau} = 2\nu_t \mathbf{S} - \frac{2}{3} k\mathbf{I} \quad (3)$$

where ν_t is the turbulent viscosity, $\mathbf{S}$ is the strain rate tensor $(1/2(\nabla \mathbf{u} + (\nabla \mathbf{u})^T))$, k is the turbulent kinematic energy and $\mathbf{I}$ is the identity matrix.

In order to specify the turbulent viscosity ν_t and to close the above equations, the k-ω SST model (Menter, 1994) is used in the current model, as it combines the advantages of the original k-ω model (Wilcox, 2006) near walls and k-ε model (Jones and Launder, 1973) away from wall. A detailed description of the k-ω SST model refers to Menter (1994).

2.2 Free surface tracking

In OpenFOAM, the volume of fluid (VOF) method is used to capture the free surface. The VOF method was proposed by Hirt and Nichols(1981), in which a volume fraction α was defined in a manner that α = 0 corresponds the air phase and α =1 represents the water phase, and intermediate value is a mixture of the two fluids. Here α=0.5 is regarded as the free surface. The volume fraction can be determined by solving the advection equation:

$$\frac{\partial \alpha}{\partial t} + \nabla \times (\alpha \mathbf{u}) + \nabla \times (\alpha(1-\alpha)\mathbf{u}_r) = 0 \quad (4)$$

where $\mathbf{u}_r$ is a relative compression velocity. The variations of any fluid property, such as μ and ρ, are expressed as functions of α:

$$\rho = \alpha\rho_1 + (1-\alpha)\rho_2 \tag{5}$$

$$\mu = \alpha\mu_1 + (1-\alpha)\mu_2 \tag{6}$$

where ρ_1 and μ_1 are the density and the dynamic viscosity of water; ρ_2 and μ_2 are the density and the dynamic viscosity of air.

2.3 Wave generation

The second order Stokes waves are generated in the current model utilizing the waves2Foam developed by Jacobsen et al. (2012). The free surface elevation η is given by:

$$\eta = \frac{H}{2}\cos(kx-\omega t) + \frac{H^2k}{16}\frac{\cosh kh}{\sinh^3 kh}(2+\cosh 2kh)\cos\left[2(kx-\omega t)\right] \tag{7}$$

where H is the wave height, h is the water depth, ω is the wave angular frequency and k is the wave number.

3. Validation of the numerical model

3.1 Experimental set-up

In this section, in order to validate the OpenFOAM model on problems concerned, the numerical results of regular wave propagation and overturning over a submerged reef with steep slope are compared with experimental data. The sketch of the experimental arrangement is shown in Fig. 1. The flume is 69.0 m long, 2.0 m wide and 1.8 m deep. The submerged reef slope is 1:5 and the height of the reef is 0.5m. The mean water depth is h_0=0.715m. Wave data are measured by 17 wave gauges at different locations

along the wave flume: wave gauges 1–3 are located before the steep slope, 4–10 are located at the slope, 11 is at the edge of the reef flat, and 12–17 are arranged on the reef flat. Three incident wave cases are used in the test, which are listed in Table 1. These three waves have the same wave period T=2.0s but different wave heights H= 0.10m, 0.14m and 0.20m. They represent the spilling breaker, plunging breaker and violently plunging breaker, respectively.

3.2 Numerical set-up

Fig. 2 shows a sketch of the numerical setup. In order to reduce the computational time, the numerical wave flume is 38.5m long and 1.015m high. The reef flat edge is at the location 14.5m away from wavemaker, which is a little shorter than that in the experiment. The length of the reef flat is 24.0m. According to the physical experiment, the water depth is 0.715m with the reef flat water depth being 0.215m. Two relaxation zones of 4.0m long are set both at the front and the end of wave flume to avoid wave reflection. Two different computational meshes are used in the current simulation, and the mesh parameters are listed in Table 2. In front of the reef, the water depth is deeper and the wave nonlinearity is relatively weaker, and thus the coarse mesh A was used. The average grid size in X direction and Y direction are Δx=0.02m and Δy=0.005m, respectively. The number of points per wavelength and points per wave height are $p.p.w$=223 and $p.p.w.h \geq 16$, respectively. Near the reef plat, because the wave nonlinearity is stronger and the breaking is violent, the fine mesh B with Δx=0.01m and Δy=0.005m, is used to simulate the high order harmonic wave components and the violent wave motion. In addition, in order to ensure the accuracy and stability of the model, the maximum Courant number $Co = \Delta t|U|/\Delta x$ is set to 0.2 throughout the computational domain.

On the bottom boundary, the no-slip boundary condition is considered for the velocity *U*. And on the top and the right boundaries, the Neumann boundary condition is applied. For the *k*-*ω* SST model, the turbulence kinetic energy *k* and turbulent frequency *w* are set to constant values on the inlet patch. In particular, *k* is computed based on the turbulence intensity *I* which is estimated to be 1%. The value of *k* on the inlet is expressed as $k=3/2(U_{\max}I)^2$ ($U_{\max}$ is the maximum wave velocity), and the value of *w* is calculated according to $w=\sqrt{k}/h$, where *h* is water depth *h*=0.715m. On the bottom boundary, *k* was set to 0 and *w* is calculated using the wave depth on the flat, i.e. *h*= 0.215m.

3.3 Free surface elevations

The comparisons of free surface time series between the numerical results and experimental data for three cases are presented in Figs. 3-5. It can be seen that good agreements have been achieved between the numerical and experimental results for all three cases. For case A, the wave height is the smallest one. The surfaces maintain the shape of monochromatic wave at the locations in front of the reef (see 1# and 4#). At locations 6# and 12#, the free surface shows an asymmetric form owing to wave shoaling. In particular, when the wave is propagating on the reef flat, obvious nonlinear phenomena can be observed. The wave crests become steep and wave troughs become flat. At location 15#, the free surface becomes unstable and wave height decreases because of the wave breaking. Stronger wave nonlinearity is observed at location 16# after wave breaking. The whole process, including wave shoaling, wave breaking and strong nonlinear interactions, is well captured by the numerical model. For case B and C (see Figs. 4 and 5), despite that there are larger breakers and stronger nonlinear interactions, the numerical model still predicts the free surface elevations well,

compared to the experimental measurements.

3.4 Wave height and wave setup

Fig. 6 shows the comparisons of the average wave heights between numerical results and experimental data for these three cases. At the locations in front of reef, because of the reflection of the reef, wave heights are fluctuant. Thus, the wave heights listed in Table 1 are the results measured at location 1#, rather than the values inputted at the wavemaker in the experiment. For instance, in case A, the input wave height value is 0.093m. When wave propagates on the reef flat, wave heights become larger due to wave shoaling, before wave breaking occurs. After wave breaking, wave heights decrease significantly due to energy dissipation. From Fig. 6, it can also be seen that the present numerical model predicts the wave height accurately.

Wave breaking also causes mean water level change. Usually, the mean water level increasing after wave breaking and decreasing before wave breaking are called wave setup and setdown, respectively. For short, the whole phenomenon is often denoted as wave set-up. Here, the setup is calculated using the average of free surface values over time: $\bar{\eta}(t)$. Fig. 7 shows the wave setup at different locations for these three cases. It can be found that there are wave setups on the reef flat after wave breaking point, and there exists setdown in front of the reef slope due to the requirement of conservation of mass. The comparisons between the numerical and experimental results show good agreement, demonstrating that the present numerical model is capable of predicting the wave setup on the reef flat.

3.5 Harmonic components

Wave propagation over submerged reef involves strong nonlinear processes. In order to

demonstrate the accuracy of the numerical model for simulating the strong nonlinear waves, the comparisons between the numerical and experimental wave harmonic components at different locations for the three cases are shown in Figs. 8-10. In these figures, wave harmonic components up to 4^{th} order are given, and the amplitudes of each component A_i are normalized by the initial wave amplitude A_0. The variation of the harmonic components during the wave propagation and transformation can be seen from these figures. It is seen that at the locations in front of reef, the first order component dominates. As waves propagate over the reef slope, amplitudes of the higher order components increase significantly due to wave shoaling and nonlinear process; even the 4^{th}-order components can be observed. After wave breaking, the amplitudes of each component decrease due to energy loss. It can be found that the wave energy dissipation due to wave breaking is mainly from the first harmonic components. For case A, which has a weak breaker, the amplitude of the first order components reduces by 60%. While, for case C, which has a violently breaker, the first order components reduces by 80%. Compared to the first order components, the higher order components have smaller loss of wave amplitude during wave breaking. From the free surface elevations, it can also be seen that the wave crest becomes steep and the wave trough becomes flat. In general, here good agreements have been obtained between the numerical and experimental results, which further confirm that the present numerical model is capable of capturing high order components in these complex scenarios.

4. Numerical investigation of the effect of wave height, slope and submergence of the reef

To further investigate the properties of wave transformation on the reef topography, various wave heights, slopes and submergences of the reef are considered and simulated. Three different slopes tanα are adopted: 1:2, 1:5 and 1:15, respectively. The height of

the reef is 0.5m and three different submergences are used: the submergences h_r = 0.125m, 0.215m, and 0.335m, corresponding to the deep water h_0 = 0.625m, 0.715m, and 0.835m, and water depth ratio, $\varepsilon = h_r/h_0$ = 0.2, 0.3, and 0.4, respectively. A series of monochromatic wave with various wave heights H_0 from incipient breaker to violent breaker were generated. The wave conditions are listed in Table 3.

4.1 Reflection coefficients and transmission coefficients

The reflection coefficient K_r and transmission coefficient K_t are defined by the following equations:

$$K_r = \frac{H_r}{H_0}, \quad K_t = \frac{H_t}{H_0} \tag{8}$$

where, H_0 is the incident wave height and H_r is reflected wave height by the reef topography. The reflected wave height is separated using the two-point method proposed by Goda(2010). H_t is the wave height of the transmitted wave over the reef flat. It should be pointed out that during the wave propagation on the reef flat, the wave height decreases due to wave breaking and bottom friction. Furthermore, it is observed that wave breaking occurs within three wavelengths from the edge of the reef. Here, mainly considering the influence of wave breaking, the wave heights at the locations three times the wavelength behind the breaking point are adopted to represent the transmitted wave heights.

Fig. 11 shows the reflection coefficients as a function of the deep-water wave steepness H_0/L_0 (L_0 is the wave length in deep water) for different reef slopes with fixed water depth ratio ε = 0.3. It can be seen that the variation of the reflection coefficient with the wave steepness keeps almost constant. That means that the wave steepness affects the reflection coefficient very slightly. However, the reef slope has a significant

influence on the wave reflection. The reef with a steeper slope leads to larger wave reflection. In particular, when the reef slope is 1:2, the reflection coefficient is approximately 15%. However, when the reef slope is small (1:15), its reflection is also small. Moving to the wave transmission coefficient as shown in Fig. 11(b), it can be seen that the reef slope has a slight influence on the wave transmission coefficient. This means that the transmission wave heights are almost same after wave breaking for different slopes, which is due to the fact that the water depths on the reef flat are identical water depths. Nevertheless, it is worth noting that the transmission coefficient decreases as the incident wave steepness increases.

Fig. 12 presents the influence of reef submergence on the reflection coefficients and transmission coefficients. Here, a non-dimensional submergence parameter $(\bar{\eta}+h_r)/H_0$ is used to represent the relative submergence, where $\bar{\eta}$ is the wave induced setup. Generally, shallower submergence causes larger wave reflection. However, in Fig. 12(a), the values of reflection coefficient for water depth ratio ε = 0.2 are smaller than those for ε = 0.3. This may be because the water depth is too shallow, and thus the wave breaking may affect the wave reflection and reduce the wave energy of the reflected wave. In Fig. 12(b), as expected, deeper water depth allows larger wave to propagate on the reef flat. So, the transmission coefficients for larger relative submergence are greater.

4.2 Breaking wave height

To understand the breaking wave height, as an example, Fig. 13 compares wave height variations over different slopes for the cases with fixed wave height H_0=0.16m. It can be seen that as the reef slope becomes steeper, the wave height variation along the topography fluctuates in the region in front of the reef due to the larger wave reflection.

As the reef slope is mild, the wave height increases gradually with wave shoaling on the slope. In Fig. 13, it is also observed that the breaking wave heights are almost the same. However, the breaking points are shifted slightly towards deep water as reef slope becomes milder. This indicates that the breaking wave heights are similar for different slopes, but the water depths at breaking point are different.

The relative breaking wave height defined as the ratio of the breaking wave height H_b and incident wave height H_0 in deep water, is an important criterion to describe the breaking wave height. Fig.14 gives the relationship between the relative breaking wave height and deep-water wave steepness H_0/L_0 for all the simulated wave cases. The theoretical results of Munk(1949), the modified Munk's formular by Komar and Gaughan(1972) and the empirical formula from the experimental study by Xu et al.(2018) are also given in the figure for comparison. It clearly shows that the relative breaking wave height depends on the deep-water wave steepness. But the reef slope and submergence have no significant effects on relative breaking wave height. Also, it can be seen that the numerical results deviate significantly from the results of Munk (1949). While, it has good agreements with the empirical formula of Xu et al. (2018) and Komar and Gaughan (1972), especially for the results of Xu et al. (2018).

Although wave breaking heights are similar to the waves with the same H_0/L_0, the breaking water depths are different as mentioned above. Fig. 15 and Fig. 16 show the comparisons of the ratios between breaking wave height and breaking depth H_b/h_b for different slopes and different submergences, respectively. In Fig. 15, when the incident wave heights are smaller ($H_0/L_0<0.024$), the waves break on the reef flat, H_b/h_b increases as H_0/L_0 increases. Also, it is seen that for these small waves the slope of the reef has very slight influences on H_b/h_b. This hints that reef slope has no significant influences on the breaking depth when the wave breaks on the reef flat. However, when

the incident wave becomes larger (H_0/L_0>0.024), the wave breaking occurs above the slope, it is seen that H_b/h_b is heavily influenced by the reef slope. In particular, for steep slopes H_b/h_b still increases as H_0/L_0 increases. However, for mild slope (1:15), H_b/h_b slightly decreases as H_0/L_0 increases. This indicates that the reef slope can strongly affect the breaking depth for large waves (H_0/L_0>0.024) in these test cases.

In Fig. 16, it appears that the value of H_b/h_b decreases with increasing non-dimensional submergence parameter $(\bar{\eta}+h_r)/H_0$. It can also be found that the submergence has significant influence on the value of H_b/h_b. That is H_b/h_b decreases with increasing non-dimensional submergence parameter. For all the numerical test cases, the minimum value of H_b/h_b is 0.56, which is close to the result reported in Nelson (1983) that the H_b/h_b will not excess 0.55 for stable waves. This implies that the threshold of the ratio between the maximum breaking height and water depth for wave breaking is about 0.56.

4.3 Wave setup

The influences of the reef slope and submergence on the wave induced setup are illustrated in Fig.17 and Fig.18, respectively. Fig. 17 shows that the wave setups on the reef flat with different reef slopes are almost the same. This is because the three cases have similar breaking range owing to the almost same breaking wave heights. However, the wave setdown in surf zone is different for various reef slopes. The waves propagating on steeper slope can cause larger setdown. In Fig. 18, it can be seen that the wave setup is obviously dependent on the reef submergence. With the shallower submergence, larger wave setup occurs.

Further, Fig. 19 gives the variation of the non-dimensional wave setup $\bar{\eta}/(T\sqrt{gH_0})$ and the non-dimensional submergence considering the wave setup

$(\bar{\eta}+h_r)/H_0$ for all the numerical cases. The setup values at the location three times the wavelength behind the breaking point are adopted to represent the setup value at the reef flat. The figure shows that there are strong correlations between the wave setup and submergence. The wave setup increases with decreasing non-dimensional submergence. In this figure, numerical results are compared with experimental data from Xu et al. (2018) and Gourlay (1996). It can be found that the numerical results are agreed with experimental data well. Based on this data, a fitting curve that predicts the wave setup can be written as:

$$\frac{\bar{\eta}}{T\sqrt{gH_0}} = 0.0084\left(\frac{\bar{\eta}+h_r}{H_0}\right)^{-2.604} \tag{9}$$

The formula indicates that the wave induced setup on the reef flat is mainly controlled by reef submergence and wave height for fixed wave period.

4.4 Energy dissipation

According to the conservation of energy, the energy dissipation during wave propagating over the reef can be expressed as

$$P_d = P_0 - P_r - P_t \tag{10}$$

where, P_d is the energy flux loss during the wave propagation, which is caused by wave breaking and bottom friction. P_0 is the energy flux of incident wave. P_r and P_t are the energy flux of reflected wave and transmission wave, respectively.

Wave energy flux P_0, P_r and P_t can be written as following:

$$P_0 = \frac{1}{8}\rho g H_0^2 C_{g0} \tag{11}$$

$$P_r = \frac{1}{8}\rho g H_r^2 C_{gr} = \frac{1}{8}\rho g K_r^2 H_0^2 C_{gr} \tag{12}$$

$$P_t = \frac{1}{8}\rho g H_t^2 C_{gr} = \frac{1}{8}\rho g K_t^2 H_0^2 C_{gt} \tag{13}$$

where, C_{g0}, C_{gr} and C_{gt} are the wave group velocity corresponding to incident wave, reflected wave and transmission wave, respectively. They are estimated by the formula $C_g = \omega^{'} / k(1+2kh/sh2kh)$,where $\omega^{'}$ is wave angular frequency and k is wave number.

Fig. 20 gives the relationships between the energy reflection rate(P_r/P_0), energy transmission rate(P_t/P_0), energy dissipation rate(P_d/P_0) and deep-water wave steepness H_0/L_0 for different reef slopes. From Fig. 20(a), it can be seen that the energy reflection rate is very small, and most of the energy travels forward. The same result can be achieved from Fig. 11. From Fig. 20(b) and (c), it can be found that most of energy is consumed during wave breaking process. As expected, the energy dissipation rate increases with increasing deep-water wave steepness. The larger incident wave has stronger breaker and more energy loss on the reef. In addition, the energy dissipation rate is almost the same for different reef slopes when the wave steepness is big because the breaking wave height for different slope are almost the same, all three cases have similar breaking range and energy dissipation. While, when the wave steepness is small, there is a little difference between the energy dissipation for different reef slopes. This is because the energy dissipation is mainly caused by bottom friction when the wave height is small. The milder slope which has longer slope face increases the energy dissipation.

Similar to Fig. 20, the variation of energy reflection rate(P_r/P_0), energy transmission rate(P_t/P_0) and dissipation rate(P_d/P_0) with the relative submergence are given in Fig. 21. It also shows that the wave reflection is weak during wave propagation.

And there are strong correlations between energy transmission rate and dissipation rate with relative submergence. Because larger submergence, which has deeper water depth on reef flat, can support larger wave height. It means less energy would lose during the wave breaking. So, in Fig.21 (b) and (c), it can be found that the energy transmission rate increases and the energy dissipation rate decreases with non-dimensional submergence increasing. And similar phenomenon can be observed for all the three different water depth ratio ε.

5. Conclusions

The numerical model for simulating wave propagation over a submerged reef has been established using OpenFOAM based on the Reynolds averaged Navier-Stokes equations together with VOF and *k*-*w* SST turbulence model. It is verified by the comparisons of the numerically simulated wave surface elevation, wave height, wave setup and harmonic component with experimental results. The numerical model was reliable to simulate the process of wave shoaling, breaking and transmission on the reef. Further, a series of numerical experiments are conducted considering various reef slope and submergence of reef. The influences of reef slope and submergence on wave reflection and transmission, breaking wave height, wave setup and energy dissipation during wave propagation on the reef have been investigated and analyzed. The main conclusions from the numerical studies are:

(1) The reef slope can significantly affect wave reflection coefficient. The reef with steeper slope generates larger reflected wave. Reef submergence has obvious influence on the transmission coefficient. The transmission coefficient increases with increasing non-dimensional submergence parameter $(\bar{\eta}+h_r)/H_0$.

(2) The maximum breaking wave height can be predicted by breaking criteria H_b/H_0 proposed by Xu et al. (2018). The breaking water depth is influenced by reef slope and non-dimensional submergence. As wave breaking occurs on the reef slope face, the ratios between breaking wave height and breaking depth H_b/h_b become larger when the slope is deeper. And the value of H_b/h_b slightly decreases as $(\bar{\eta}+h_r)/H_0$ increasing. In all the cases presented, the minimum value of H_b/h_b is 0.56. It implies that the threshold of the ratio between maximum breaking height and water depth for wave breaking is about 0.56.

(3) The wave induced setup on the reef flat is mainly controlled by the reef submergence and the incident wave steepness. Based on the present numerical results and previous experimental data, an empirical formula is proposed to predict the wave induced setup on the reef flat.

(4) The submergence also affects the energy loss during wave propagating on the reef. The energy dissipation rate decreases almost linearly as the non-dimensional submergence $(\bar{\eta}+h_r)/H_0$ increasing.

Acknowledgements

This work was financially supported by State Scholarship Fund of China (No. 201606065013), the National Natural Science Foundation of China (Grant No. 51579038), the National Basic Research Program (Grant Nos. 2013CB036101), the Fundamental Research Funds for the Central Universities and the Fundamental Research Project for Key Laboratory of Department of Liaoning Province. Their supports are gratefully acknowledged.

References:

Alagan Chella, M., Bihs, H. & Myrhaug, D. [2015] "Characteristics and profile asymmetry properties of waves breaking over an impermeable submerged reef," *Coastal Engineering*, 100, 26-36.

Blenkinsopp, C. E. & Chaplin, J. R. [2008] "The effect of relative crest submergence on wave breaking over submerged slopes," *Coast. Eng*. 55(12), 967-974.

Chen, G., Kharif, C., Zaleski S. & Li, J. [1999] "Two-dimensional Navier–Stokes simulation of breaking waves," *Phys. Fluids* 11(1), 121-133.

Chen, L. F., Zang, J., Hillis, A. J., Morgan, G. C. J. & Plummer, A.R. [2014] "Numerical investigation of wave–structure interaction using OpenFOAM," *Ocean Engineering* 88, 91–109.

Chenari, B., Saadatian, S. & Ferreira, A. D. [2015] "Numerical modelling of regular waves propagation and breaking using waves2foam," *Journal of Clean Energy Technologies* 3(4), 276-281.

Devolder, B., Troch, P. & Rauwoens, P. [2018] "Performance of a buoyancy-modified k-ω and k-ω SST turbulence model for simulating wave breaking under regular waves using OpenFOAM®," *Coastal Engineering*, 138, 49-65.

Fang, K., Yin, J., Liu, Z., Sun, J. & Zou, Z. [2014] "Revisiting study on Boussinesq modeling of wave transformation over various reef profiles," *Water Science and Engineering* 7(3), 306-318.

Goda, Y. [2010] "Random seas and design of maritime structures," *World scientific*.

Gourlay, M. R. [1994] "Wave transformation on a coral reef," *Coast. Eng.* 23, 17-42.

Gourlay, M. R. [1996] "Wave set-up on coral reefs. 1. Set-up and wave-generated flow on an idealized two dimensional horizontal reef," *Coast. Eng*. 27, 161-193.

Hardy, T. A. & Young, I. R. [1991] "Wave attenuation on an offshore coral reef," *Journal of Geophysical Research Atmospheres* 101(C6), 14311-14326.

Hieu, P. D., Katsutoshi, T. & Ca, V.T. [2004] "Numerical simulation of breaking waves using a two-phase flow model," *Appl. Math. Model* 28(11), 983-1005.

Higuera, P., Lara, J. L. & Losada, I. J. [2013] "Simulating coastal engineering processes with OpenFOAM®," *Coast. Eng.* 71, 119-134.

Hirt, C. W. & Nichols, B. D. [1981] "Volume of fluid (VOF) method for the dynamics of free boundaries," *J. Comput. Phys.* 39(1), 201-225.

Jacobsen, N. G. & Fredsoe, J. [2014] “Formation and development of a breaker bar under regular waves. Part 2: Sediment transport and morphology,” *Coast. Eng.* 88, 55-68.

Jacobsen, N. G., Fuhrman, D. R. & Fredsøe, J. [2012] “A wave generation toolbox for the open-source CFD library: OpenFoam®,” *Int. J. Numer. Meth. Fl.* 70(9), 1073-1088.

Jensen, O. [1991] “Waves on coral reefs,” *Proc. 7th Symp. Coastal and Ocean Management*, Long Beach, 3, 2668–2680.

Jones, W. P. & Launder, B. E. [1973] “The calculation of low-Reynolds-number phenomena with a two-equation model of turbulence,” *Int. J. Heat Mass Tran*. 16(6), 1119-1130.

Karambas, T. V. & Koutitas, C. [2002] “Surf and swash zone morphology evolution induced by nonlinear waves,” *J. Waterw. Port Coast.* 128(3), 102-113.

Kim, D. H. [2015] “H2D morphodynamic model considering wave, current and sediment interaction,” *Coast. Eng*. 95, 20-34.

Kirby, J. T. [2016] “Boussinesq Models and Their Application to Coastal Processes across a Wide Range of Scales,” *J. Waterw. Port Coast.* 142(6), 03116005.

Komar, P. D. & Gaughan, M. K. [1972] “Airy wave theory and breaker height prediction,” *Proceeding of the 13th Coastal Engineering Conference*, Vancouver, B.C. (Canada), 405-418.

Lee, J. I., Shin, S. & Kim, Y.T. [2014] “Experimental and numerical studies on wave breaking characteristics over a fringing reef under monochromatic wave conditions,” *The Scientific World Journal*. Article ID 570325, 11 pages.

Lentz, S. J., Churchill, J. H., Davis, K. A. & Farrar J. T. [2016] “Surface gravity wave transformation across a platform coral reef in the Red Sea,” *Journal of Geophysical Research: Oceans* 121(1), 693-705.

Lin, P. & Liu, P. L. F. [1998] “A numerical study of breaking waves in the surf zone,” *J. Fluid Mech.* 359, 239-264.

Lynett, P. J., Melby, J. A. & Kim, D. [2010] “An application of Boussinesq modeling to Hurricane wave overtopping and inundation,” *Ocean Eng.* 37(1), 135-153.

Massel, S. R. & Brinkman, R. M. [1999] “Measurement and modelling of wave propagation and breaking at steep coral reefs,” *Recent Advances in Marine Science and Technology* 98, 27-36.

Madsen, P. A. & Sørensen, O.R. [1992] “A new form of the Boussinesq equations with improved linear dispersion characteristics. Part 2: A slowly varying bathymetry,” *Coast. Eng.* 18(3), 183-204.

Menter, F. R. [1994] “Two-Equation Eddy-Viscosity Transport Turbulence Model for Engineering Applications,” *AIAA J.* 32(8), 1598-1605.

Morgan, G. & Zang J. [2011] “Application of OpenFOAM to coastal and offshore modeling,” *The 26th IWWWFB*, Athens, Greece.

Morgan, G., Zang, J., Greaves, D., Heath, A., Whitlow, C. & Young, J. [2010] “Using the rasInterFoam CFD model for wave transformation and coastal modeling,” *Proceedings of 32nd Conference on Coastal Engineering*. Shanghai, China.

Munk, W. H. [1949] “The solitary wave theory and its application to surf problems,” *Ann. Ny. Acad. Sci.* 51(1), 376-424.

Nelson, R .C. [1983] “Wave heights in depth limited conditions,” *Sixth Australian Conference on Coastal and Ocean Engineering*, Barton, Australia, pp. 27.

Nwogu, O. [1993] “Alternative form of Boussinesq equations for nearshore wave propagation,” *J. Waterw. Port Coast.* 119(6), 618-638.

Nwogu, O. & Demirbilek, Z. [2010] “Infragravity wave motions and runup over shallow fringing reefs,” *J. Waterw. Port Coast.* 136(6), 295-305.

Osorio-Cano, J.D., Alcérreca-Huerta, J.C., Osorio, A.F. & Oumeraci, H. [2018] “CFD modelling of wave damping over a fringing reef in the Colombian Caribbean，” Coral Reefs, 37: 1093-1108.

Peregrine, D. H. [1967] “Long waves on beach,” *J. Fluid Mech.* 27(4), 815-827.

Skotner, C. & Apelt, C.J. [1999] “Application of a Boussinesq model for the computation of breaking waves,” *Ocean Eng.* 26(10), 927-947.

Smith, E. R. & Kraus, N. C. [1991] “Laboratory study of wave-breaking over bars and artificial reefs,” *J. Waterw. Port Coast.* 117(4), 307-325.

Torres-Freyermuth, A., Lara, J. L. & Losada, I. J. [2010] “Numerical modelling of short- and long-wave transformation on a barred beach,” *Coast. Eng.* 57(3), 317-330.

Wang, Z., Zou, Q. & Reeve, D.[2009] “Simulation of spilling breaking waves using a two phase flow CFD model,” *Comput. Fluids.* 38(10), 1995-2005.

Wilcox, D. C. [2006] “Turbulence modeling for CFD,” DCW Industries: La Cañada, California, USA.

Xie, Z. [2012] “Numerical study of breaking waves by a two-phase flow model,” *International Journal for Numerical Methods in Fluids*,70(2), 246-268.

Xu, J., Liu, S. & Li, J. [2018] “Wave propagation characteristics on coral reefs,” *Journal of Hydrodynamics* (Submitted).

Yao, Y., Huang, Z., Monismith, S. G. & Lo E. Y. M. [2012] "1DH Boussinesq modeling of wave transformation over fringing reefs," *Ocean Eng.* 47, 30-42.

Yao, Y., Huang, Z., Monismith, S. G., & Lo E. Y. M. [2013] "Characteristics of Monochromatic Waves Breaking over Fringing Reefs," *Journal of Coastal Research:* 29(1): 94 – 104.

Young, I. R. [1989] "Wave transformation over coral reefs," *Journal of Geophysical Research Oceans* 94(C7), 9779-9789.

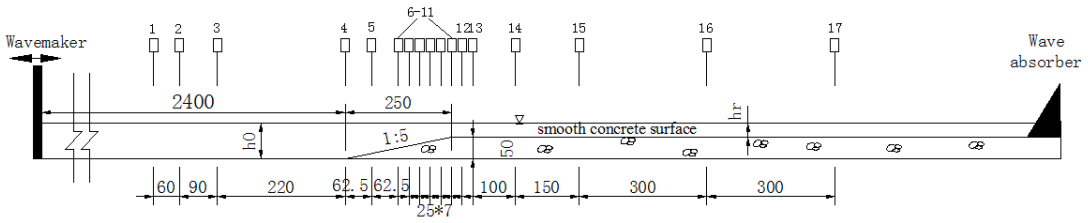

Fig. 1 The sketch of experimental set-up (Unit: cm)

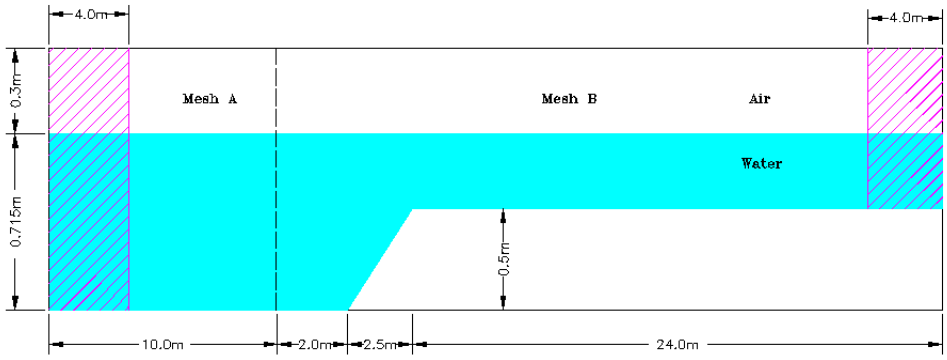

Fig. 2 The sketch of numerical set-up (Unit: m)

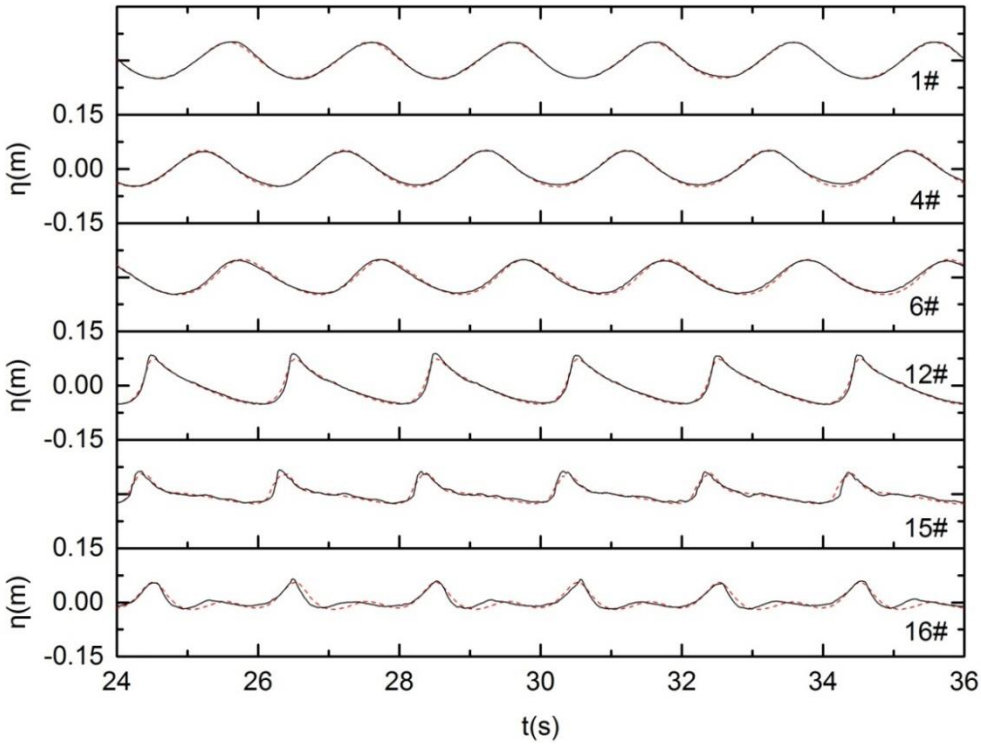

Fig. 3 Time histories of the surface elevation at different locations for case A (H=0.10m). Black solid lines: experimental results; red dashed line: numerical results.

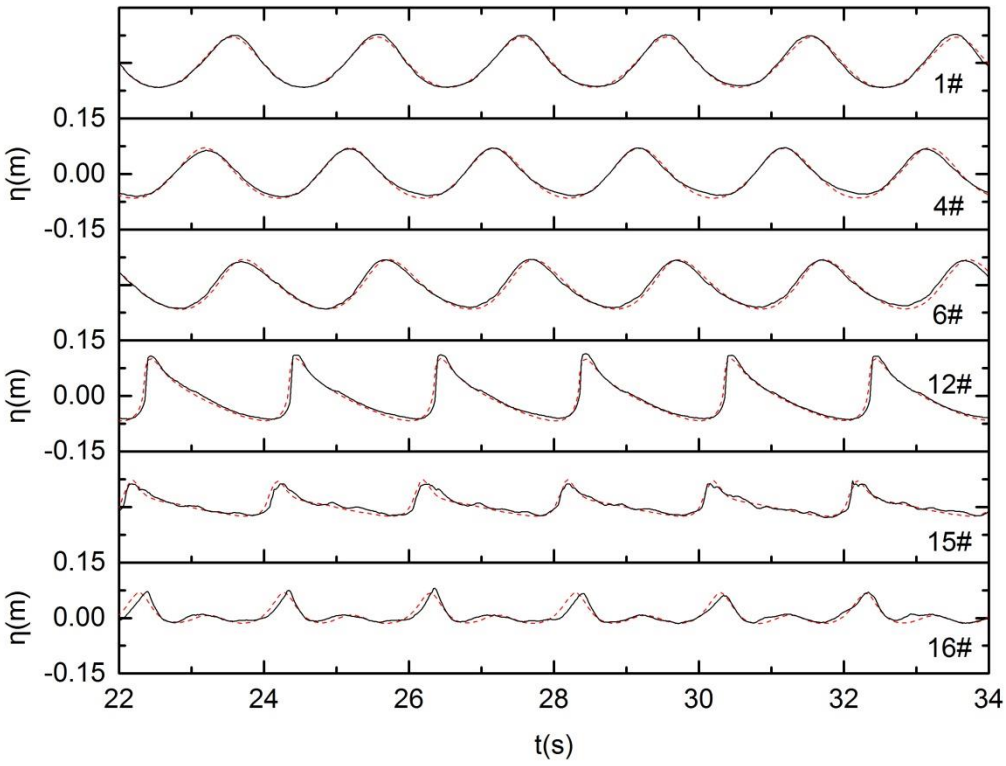

Fig. 4 Time histories of the surface elevation at different locations for case B (H=0.14m). Black solid lines: experimental results; red dashed line: numerical results.

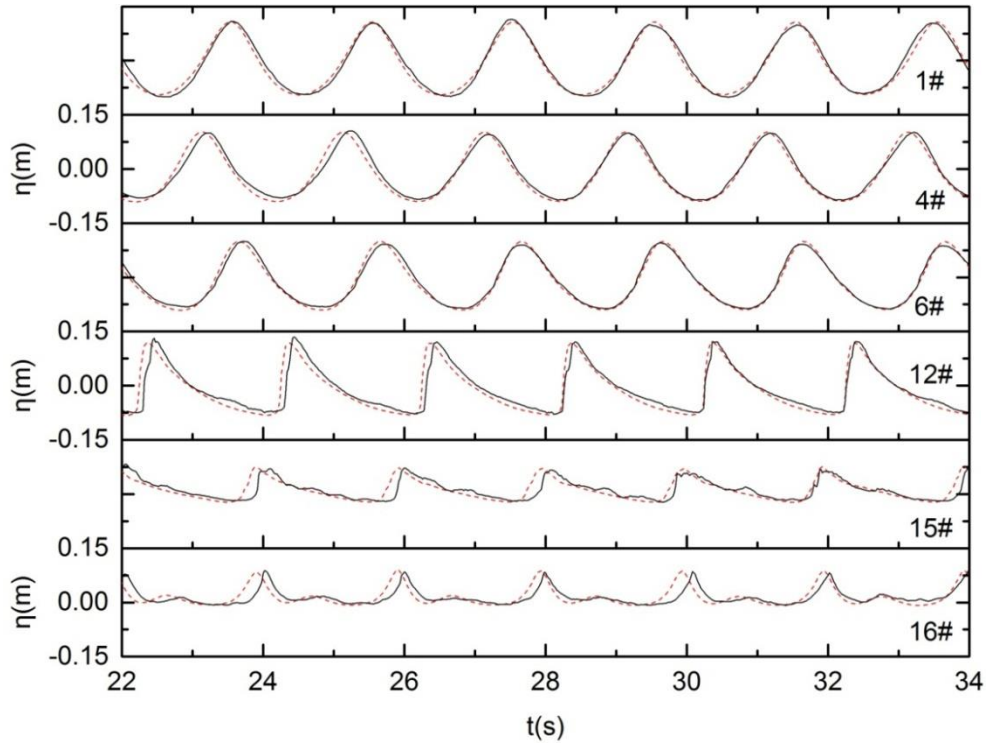

Fig. 5 Time histories of the surface elevation at different locations for case C (H=0.20m). Black solid lines: experimental results; red dashed line: numerical results.

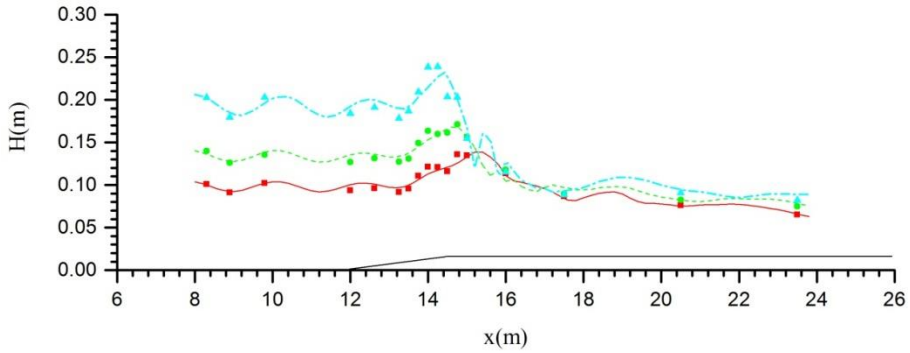

Fig. 6 The comparisons of the average wave heights between numerical results (line) and experimental results (scatter) for Case 1(red), Case 2 (green) and Case 3 (Cyan).

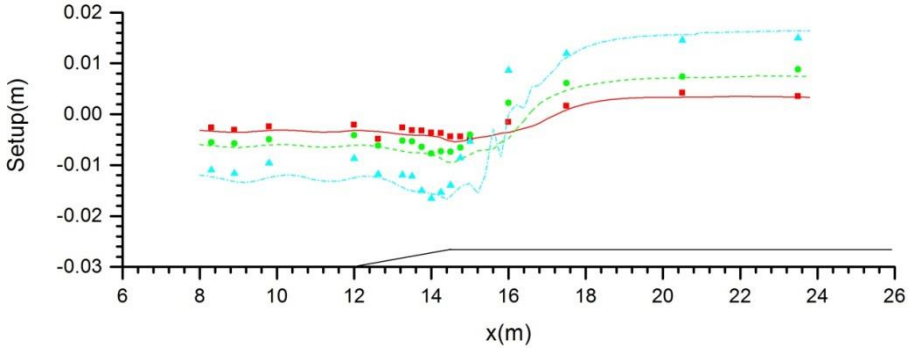

Fig. 7 The comparisons of wave setup between numerical results (line) and experimental results (scatter) for Case 1(red), Case 2 (green) and Case 3 (Cyan).

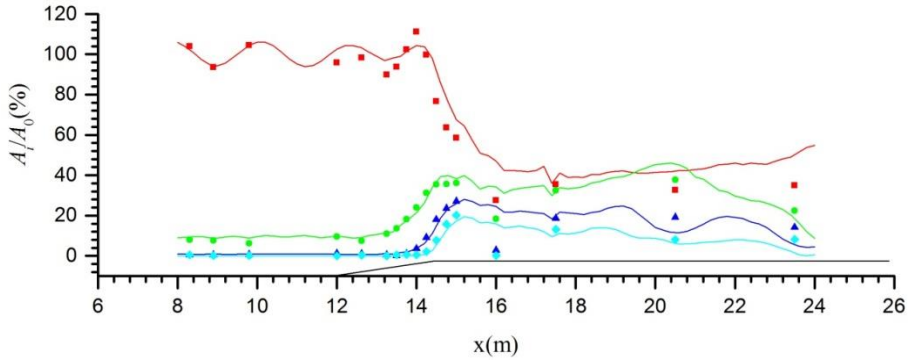

Fig. 8 Comparisons of harmonic components at different locations between numerical results (solid line) and experimental results (scatter) for case A (H=0.10m), component: 1st (red), 2nd (green), 3rd (blue) and 4th (Cyan).

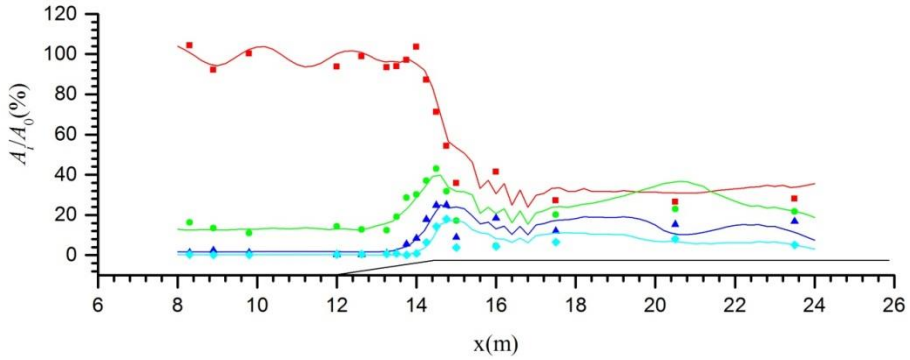

Fig. 9 Comparisons of harmonic components at different locations between numerical results (solid line) and experimental results (scatter) for case B (H=0.14m), component: 1st (red), 2nd (green), 3rd (blue) and 4th (Cyan).

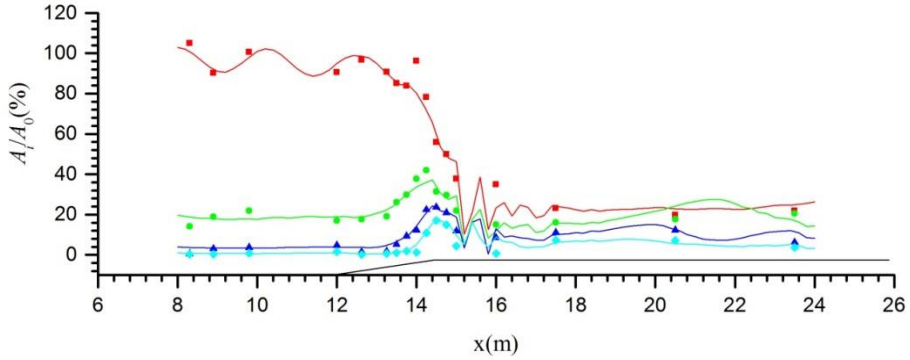

Fig. 10 Comparisons of harmonic components at different locations between numerical results (solid line) and experimental results (scatter) for case C (H=0.20m), component: 1st (red), 2nd (green), 3rd (blue) and 4th (Cyan).

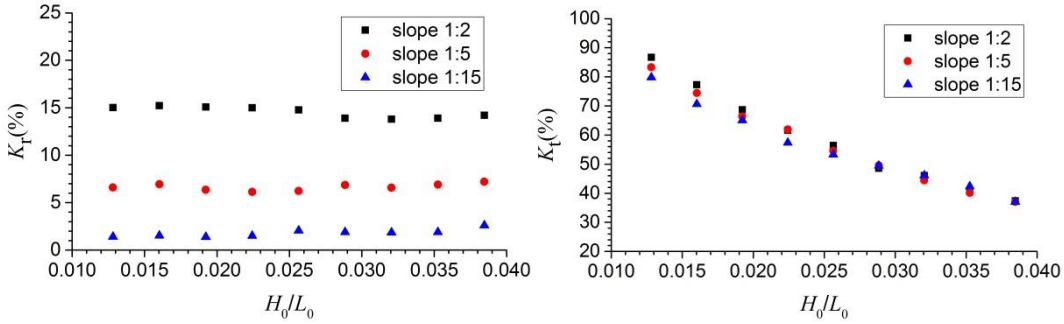

(a) reflection coefficient (b) transmission coefficient

Fig. 11 Reflection coefficients and transmission coefficients for different reef slope (ε = 0.3)

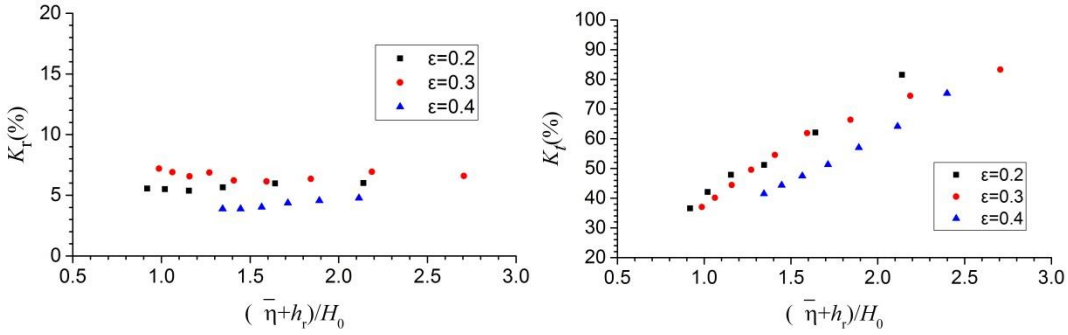

(a) reflection coefficient (b) transmission coefficient

Fig. 12 Reflection coefficients and transmission coefficients for different submergences (slope 1:5).

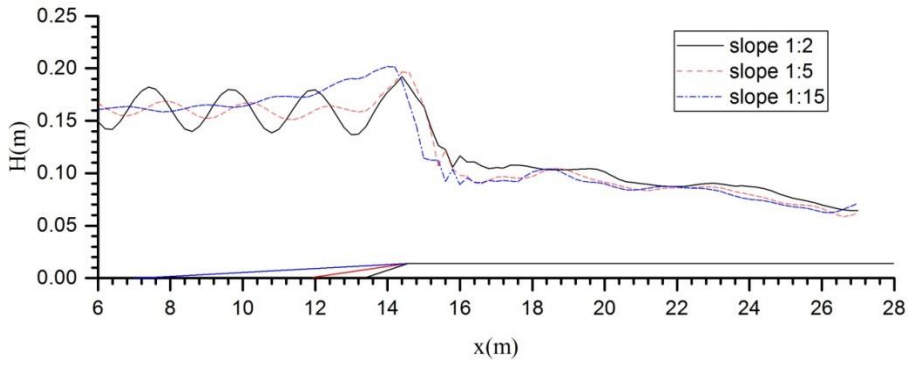

Fig. 13 Comparisons of wave height distribution for different slope (H_0=0.16m).

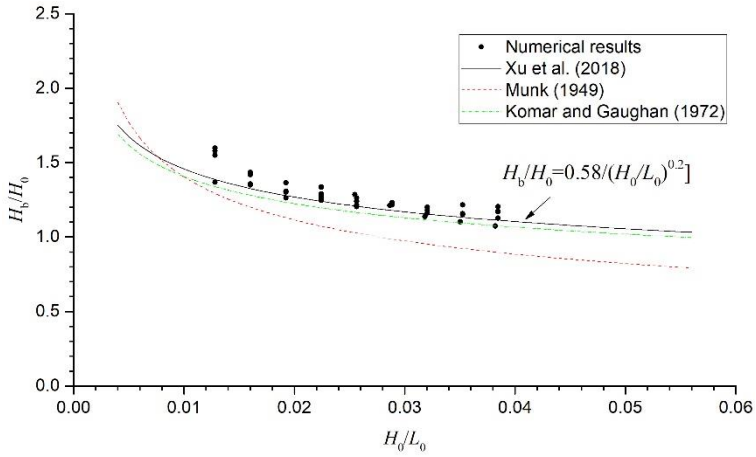

Fig. 14 Comparisons between the numerical relative breaking wave heights with the theoretical formula.

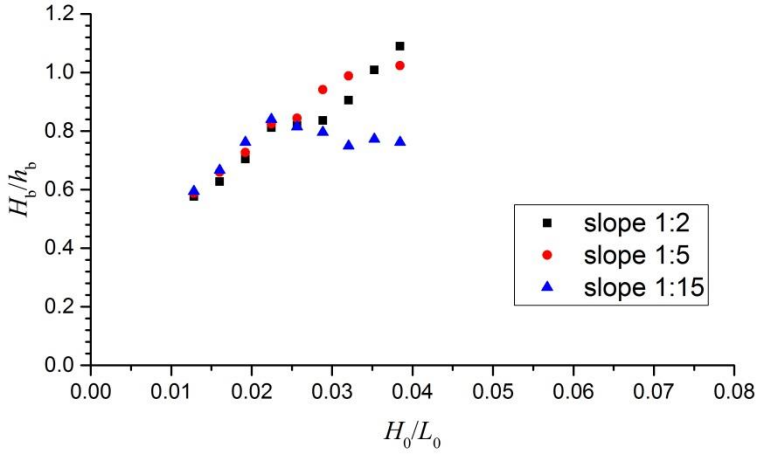

Fig. 15 Comparisons of the relative breaking wave height for different reef slopes (ε = 0.3)

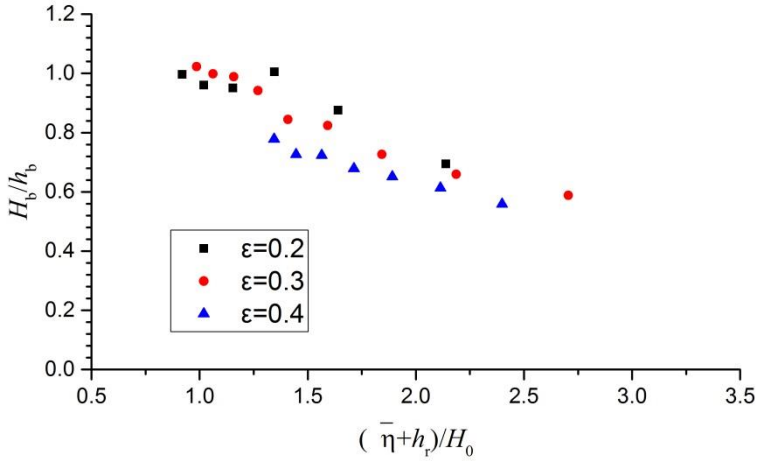

Fig. 16 Comparisons of the relative breaking wave height for different submergences (Reef slope: 1:5)

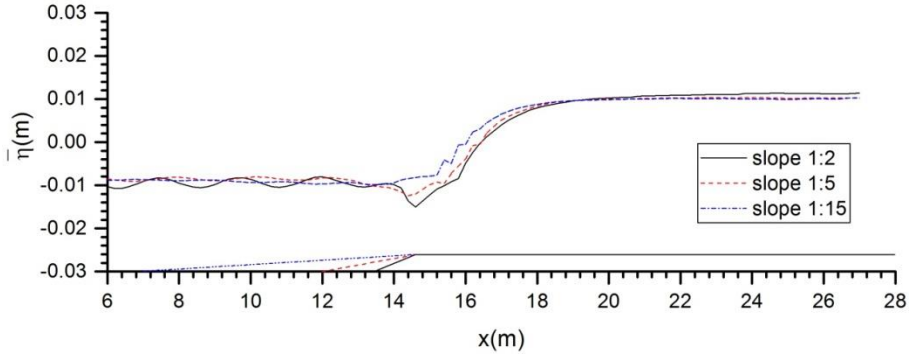

Fig.17 The comparison of wave setup for different reef slope (ε=0.3, H_0=0.16m)

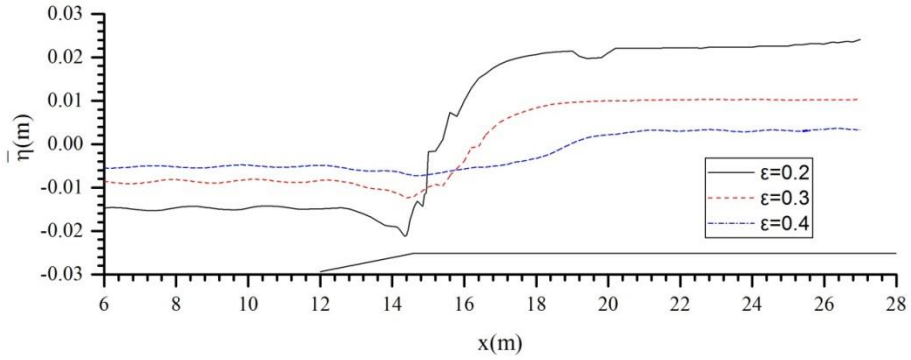

Fig.18 The comparison of wave setup for different submergences (slope: 1:5, H_0=0.16m)

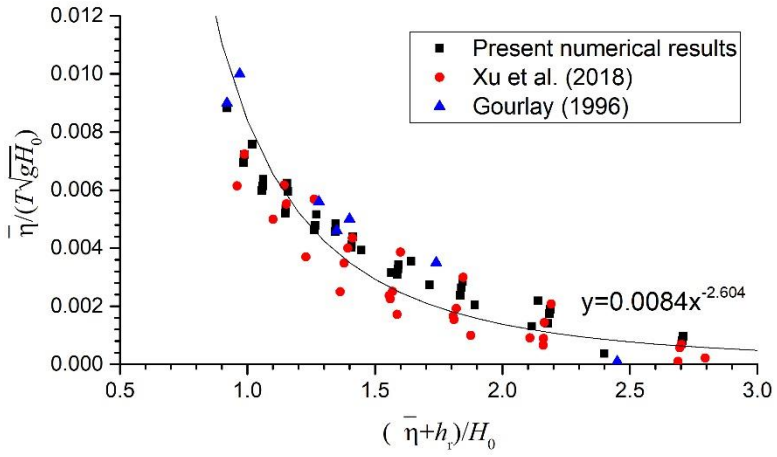

Fig.19 The relationships between the non-dimensional wave setup and submergence

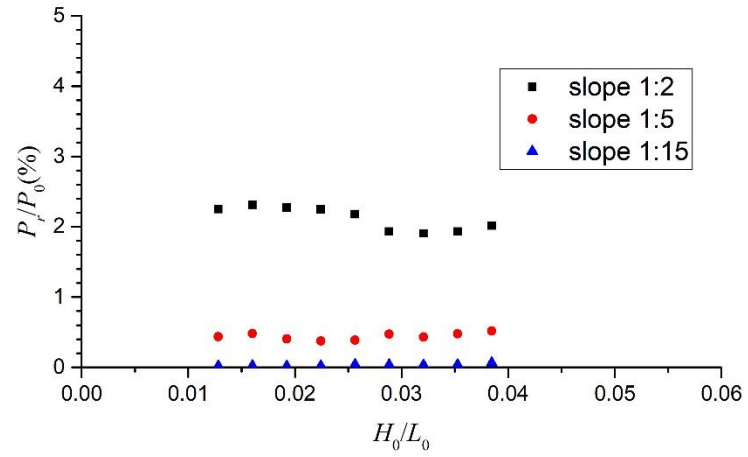

(a)

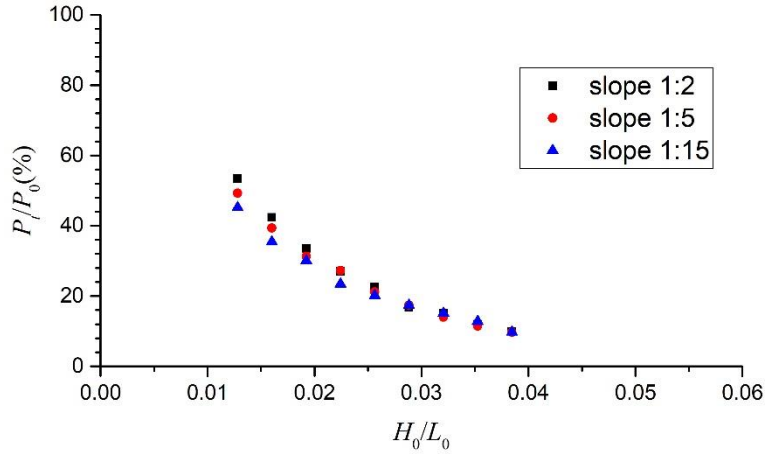

(b)

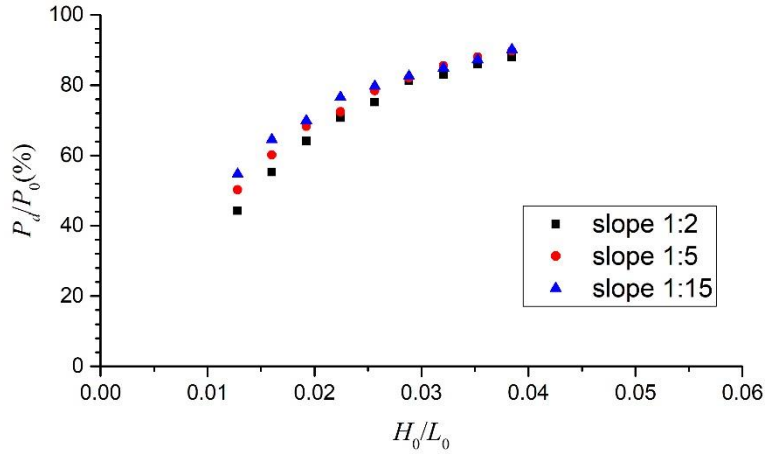

(c)

Fig. 20 The variation of energy reflection rate(P_r/P_0), transmission rate(P_t/P_0) and dissipation rate(P_d/P_0) with the incident wave steepness for different reef slopes (ε = 0.3)

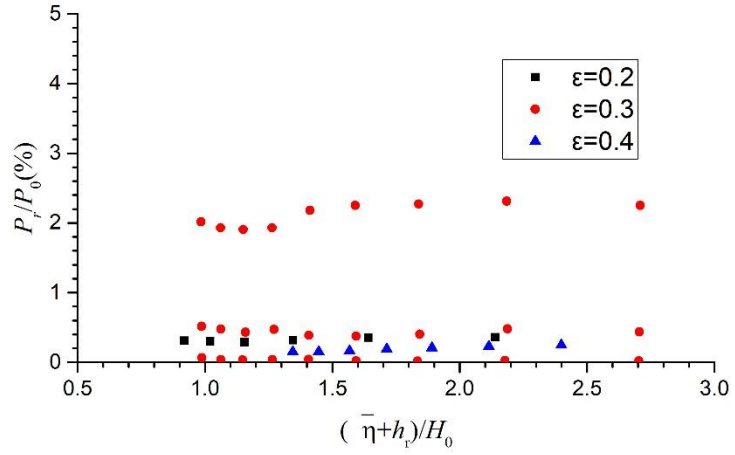

(a)

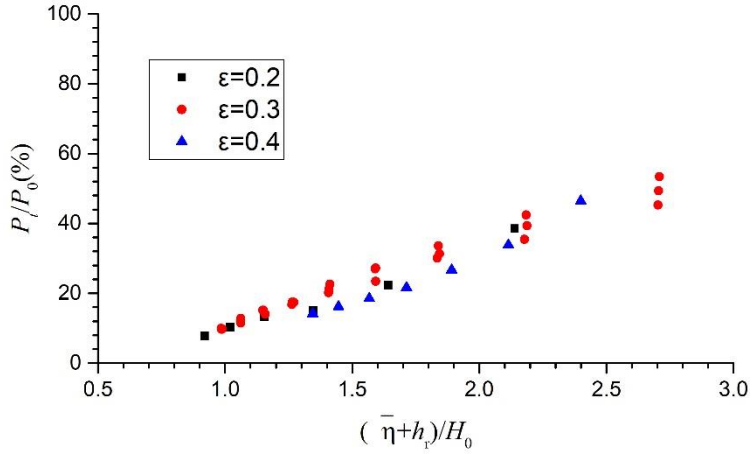

(b)

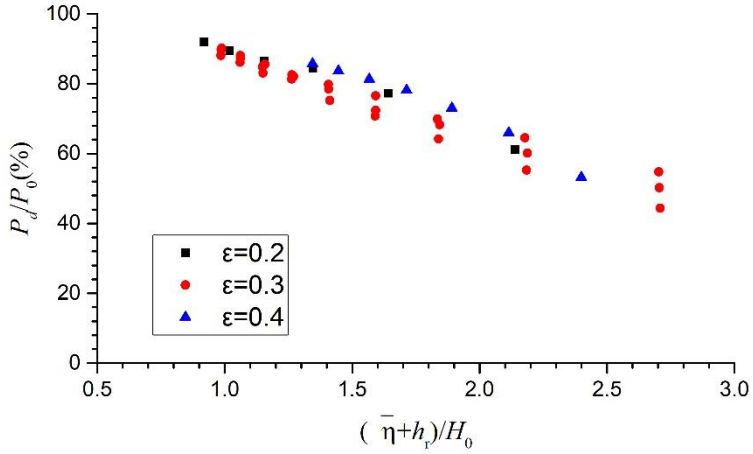

(c)

Fig. 21 The variation of energy reflection rate(P_r/P_0), transmission rate(P_t/P_0) and dissipation rate(P_d/P_0) with the relative submergence

Table 1. Experimental wave parameters.

Cases	T(s)	H(m)	$kH/2^*$	Breaker type
A	2.0	0.10	0.13	Spilling
B	2.0	0.14	0.19	Plunging
C	2.0	0.20	0.27	violently plunging

* Wave number is calculated in water depth 0.715m

Table 2. Mesh parameters.

Mesh	X direction		Y direction	
	Δx(m)	*p.p.w*	Δy(m)	*p.p.w.h*
A	0.02	233	0.005	≥16
B	0.01	466		

Table 3. The summary of wave conditions used in the numerical simulation.

h_r(m)	$\varepsilon = h_r/h_0$	tanα	H_0(m)
0.125	0.2	1:5	0.06~0.16
0.215	0.3	1:2, 1:5, 1:15	0.08~0.24
0.335	0.4	1:5	0.14~0.26